Available online at www.sciencedirect.com

SCIENCE DIRECT®

Bioelectrochemistry 65 (2004) 27–32

Bioelectrochemistry

www.elsevier.com/locate/bioelechem

Surface area involved in transdermal transport of charged species due to skin electroporation

U. Pliquett[a,*], C. Gusbeth[b]

[a] Faculty of Chemistry, Physical and Biophysical Chemistry, University of Bielefeld, D-33615 Bielefeld, Germany
[b] Institut für Hochleistungsimpuls-und Mikrowellentechnik, Forschungszentrum Karlsruhe, D-76133 Karlsruhe, Germany

Received 12 February 2004; received in revised form 5 May 2004; accepted 20 May 2004
Available online 1 August 2004

Abstract

The electroporative effect on the stratum corneum (SC) is highly localized. However, the fractional area for the transport of small ions and larger ionic species differs considerably during and after high voltage (HV) application. Electroporation of SC creates new aqueous pathways, accessible for small ions, such as Cl^- and Na^+ ions. The pores are distributed across the skin surface yielding a fractional area for current flow during electroporation of up to 0.1%. An increased permeability after high voltage application persists within a fractional area on the order of 10^{-3}%. The permeabilization of SC for larger, charged molecules (M>200 g/mol) involves Joule heating and a phase transition of the long chain sphingolipids within local transport regions (LTR). The transport area for these molecules ($\approx 10^{-3}$%) changes only negligibly after high voltage application.
© 2004 Elsevier B.V. All rights reserved.

Keywords: Transdermal drug delivery; Fractional area; Molecular transport; Stratum corneum; Electroporation

1. Introduction

The development of new drugs for medical applications faces major problems in oral or parenteral delivery. For instance, denaturation of the drug in the stomach and intestine requires major effort like encapsulation for oral delivery. The requirement of frequent delivery makes drugs unsuitable for parenteral delivery.

Transdermal drug delivery is usually limited to small, favorably lipophilic, molecules [1]. Additional driving forces like ultrasound or electric field are necessary to allow the efficient passage of larger and charged molecules [2]. Specifically, the method of skin electroporation, which creates aqueous pathways by short high electric field pulses [3], showed a transport enhancement of charged molecules like calcein (M=623 g/mol) [4] by up to four orders of magnitude. It was also estimated [5] that the surface area involved in small ion current flow was only about 0.1%. This was by two orders of magnitude larger than the area for transport of larger molecules. These estimates, however, were derived from the net transport of two fluorescent molecules and their transference numbers.

The use of fluorescence microscopy revealed that the molecular transport was highly localized [6–8]. Specifically, the transport was concentrated in circularly shaped regions with a radius in the range $50 \le r\,(\mu m) \le 300$. These localized transport regions (LTR) did not coincide with appendages or other visible defects within the structure of the stratum corneum (SC).

An increase in pulse voltage increased the density of the LTR but not their size, while longer lasting pulses produced larger LTR with negligibly small changes in the LTR-density [8]. If the pulse duration of the pulse was less than 10 μs, no LTR structures appear and the flux of calcein (M=623, z=−4) or sulphorhodamine (M=607, z=−1) was negligibly small when compared to the same total pulsing time by increasing the number of pulses [9].

By using water-soluble molecules (e.g. calcein) as polar tracers, LTR appeared in a characteristic way. The interior became dim when the SC was washed with buffer solution after pulse application. A bright fluorescing ring (calcein) remained, indicating a low permeability in the vicinity of the

* Corresponding author. Tel.: +49-521-106-6261.
E-mail address: uwe.pliquett@uni-bielefeld.de (U. Pliquett).

1567-5394/$ - see front matter © 2004 Elsevier B.V. All rights reserved.
doi:10.1016/j.bioelechem.2004.05.005

highly permeable LTR. The transport of small ions could be visualized only indirectly for Cl^- ions. A polished silver plate, serving as the anode placed behind the stratum corneum, revealed current flow by the deposition of AgCl-precipitate, seen under the microscope as gray plaque [6,10].

2. Material and methods

Human stratum corneum, either heat stripped or trypsinated, was used throughout the experiments. All the measurement methods were described previously [10,11]. The main features are as follows.

2.1. Determination of the transport area, A_{in}

The net transport of small ions across the SC was estimated from the electric current during and after the pulse application. A four-electrode system was used. At the outer electrode set a current or voltage was applied (ramp pulse or rectangular pulse) while the voltage between the inner electrodes (U_{inner}) and the total current (I) was measured. The voltage drop within the saline between the inner electrodes was used to calculate the voltage across the SC by $U_{\text{SC}} = U_{\text{inner}} - IR_{\text{saline}}$ where R_{saline} is the resistance of the saline. The control of the current rather than the voltage enables compensation for the contributions of the chemical reactions at the pulse electrodes. The apparent resistance ($R_{\text{SC}} - U_{\text{SC}}/I$) was used to calculate the surface area (A_{in}) involved in the ionic fluxes:

$$A_{\text{in}} = \rho(T) d_{\text{SC}} \frac{I}{U_{\text{SC}}} = \frac{\rho(T) d_{\text{SC}}}{R_{\text{SC}}} \tag{1}$$

where d_{SC} is the thickness of the SC and $\rho(T)$ the temperature dependent resistivity of the saline.

It was found that R_{SC} decreases during high voltage application (HV-application, $U_{\text{SC}} < 150$ V, $0.01 < t_{\text{pulse}}$ (ms) < 100). This suggested an expansion of pathways and Joule heating due to the high current density influencing A_{in}. In order to circumvent this, the values U_{SC} (100 μs) and I (100 μs), 100 μs after the beginning of a pulse, were used to calculate A_{in}. It was determined that within 100 μs the heating of the entire stratum corneum was negligible.

The SC impedance between 1 and 50 kHz before and after HV-application was measured with a time resolution of 1 ms using a time domain based arrangement [12]. A current square wave was applied to the outer electrodes and the voltage between the inner electrodes was measured. Since the current during the impedance measurements was small and the resistance of the stratum corneum was large compared to that of the saline, the voltage drop across the saline was neglected. The deformed signal was analyzed in terms of five elements, one parallel resistor and two RC-combinations, of an electric equivalent circuit [13]. Only the parallel resistor (R_{skin}) involved ionic net transport. Therefore, the post pulse A_{in} was calculated similarly to Eq. (1) but using R_{skin} instead of R_{SC}. Because the temperature during the impedance measurements remained constant, the calculation was simplified to

$$A_{\text{in}} = \frac{\rho d_{\text{SC}}}{R_{\text{skin}}} \tag{2}$$

where ρ is temperature independent.

2.2. Flux measurements and analysis

The fluxes, $J_i = (\mathrm{d}n_i)/(A\mathrm{d}t)$, of two medium sized fluorescent molecules (calcein and sulphorhodamine) were determined during 60 pulses with 1 min interpulse spacing followed by 1 h without pulsing. Even with a time resolution of 10 s, it was impossible to measure the flux during a pulse of 1 ms. For the calculation of A_{in} after the pulse Fick's first law was applied for the passive diffusion of molecules. The diffusion coefficient for calcein in water $D = 4 \times 10^{-10}$ m^2/s was estimated for 25 °C by the Stokes–Einstein equation with a radius of the hydrated molecule of 0.45 nm [14]. From the recovery phase of the flux after the pulsing, A_{in} was derived by fitting an exponentially decaying function. For the time during and between pulsing, the flux data were fitted to the Nernst–Planck equation [15]. The time-varying fractional area $A(t)/A_{\text{total}}$ for calcein is given by:

$$\frac{A(t)}{A_{\text{total}}} = \frac{J_{\text{ca}}(t) RT}{D_0 (RT + z_{\text{ca}} F U_{\text{SC}}(t))} \frac{d_{\text{SC}}}{c_{\text{ca}}} \tag{3}$$

where RT is the thermal energy, z_{ca} is the charge number calcein, F is the Faraday constant and c_{ca} is the concentration of calcein at the donor side (see Appendix A). Note, that for membrane electroporation, the degree of electroporation is defined as $f_{\text{p}} = A(t)/A_{\text{total}}$.

The flux experiments were carried out with calcein or sulphorhodamine, both were negatively charged molecules. Therefore, the anode was placed in the receiver compartment of the chamber, so that the electric field drove the molecules electrophoretically to the anode side. Macroscopically, the pathway through the SC was assumed to be homogeneous. Until a steady state is reached, the concentration (c_{donor}) of the molecules within the transport pathways results from the higher influx than efflux of fluorophores within the stratum corneum [14]. For the value of U_{SC} two cases were distinguished: one during and another between HV-application. Assuming zero electric field within the stratum corneum between the HV-applications, $U_{\text{SC}} = 0$ V. During HV-application, U_{SC} was obtained from the electrical measurements.

2.3. Qualitative measurements by imaging studies

The sites of current flow were visualized by AgCl-deposition at a polished silver anode behind the skin [6]. For the transport sites of fluorescent molecules, a special microscope chamber was used allowing the passage of the

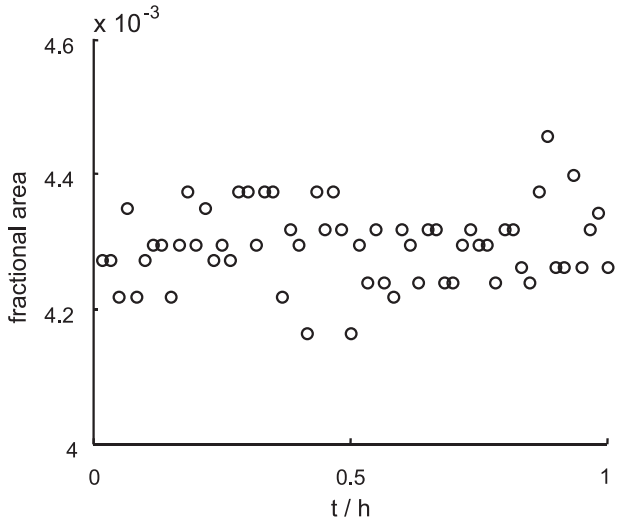

Fig. 1. Fractional surface area for the transport of small ions during the application of high voltage pulses. The surface area was determined 100 μs after the onset of the pulse using Eq. (1).

molecules to be observed during pulsing. Moreover, after the pulse protocol the skin specimen was washed and observed under the fluorescence microscope for the retained fluorophores. After several hours, the resistance distribution within the stratum corneum was again checked with the silver plate.

The temperature distribution of the skin during HV-application was visualized using temperature sensitive liquid crystals (Licristal™, Hallcrest, UK), painted directly onto the skin surface. The color was converted into temperature using a calibration between blue and red. The Licristal specifications used in these studies were designed for a temperature range between 40 and 60 °C.

2.4. Experimental results

The results show for a specific skin specimen how the surface area changed for unhindered transport of small ions and larger charged species. The specific results presented here are within the average of our experiments (about 200 similar experiments were done) and do not show any unique behavior. Since the visualization of transport could not be performed in parallel, data from experiments with the same pulse protocol but with imaged transport of either small or larger ionic species are also presented. This permits a qualitative comparison of the experimental results to facilitate the development of the proper conclusions. The mean values of transdermal transport and passive electrical behavior have been published [5,12,16].

With the onset of electroporation the apparent resistance (U_{skin}/I) of the skin dropped by several orders of magnitude which reflected the creation of aqueous pathways. From the apparent resistance 100 μs after the onset of each pulse for a 60-pulse protocol we calculated the fractional surface area (Eq. (1)) for the transport of small ions (Fig. 1), assuming a constant geometry of these pathways through the skin. The voltage across the skin was 95 V and the time constant of the exponentially decaying pulses was 1.1 ms.

Using the image at the silver plate exposed during the pulse, an involvement of the whole skin surface in current flow was found (Fig. 2). This however, does not mean, that the current density was the same throughout the skin. The temperature distribution [17] at the skin during HV-application revealed localized increased current density. Moreover, it was proven by parallel application of fluorescent dye that only the regions with temperature achieving 60 °C or more became an LTR.

The skin resistance recovered partially between pulses and continued recovery after the pulse protocol has finished. Because of the convolution between the molecular flux and the flow through the measurement apparatus, a deconvolution of the raw data was necessary [18]. Since the pulses were short (1 ms) compared to the sampling time (1 s) Dirac functions were used as modeling tools. With the use of the corrected time function for the flux, it was possible to employ Eq. (3) to calculate the fractional area for molecular transport.

As seen in Fig. 3 (upper line), there was a significant decrease of the surface area permeable to small ions after each single pulse. However, there was only negligible recovery in the fractional area involved in transport of calcein. If pores were responsible for the increased permeability, their shrinkage caused the decrease in the fractional area involved in ionic transport. This should be the same for big and small molecules. At least one would expect an effect in both cases. However, from the local distribution of the permeability after the pulse as revealed by the AgCl deposition at a silver plate (Fig. 4), we knew that the stratum corneum exhibits regions

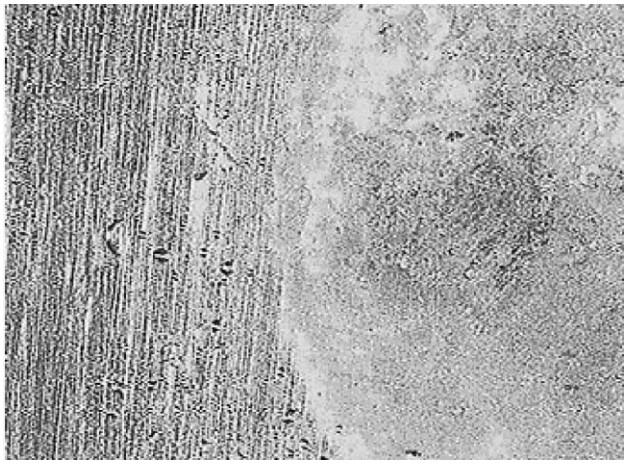

Fig. 2. Silver plate exposed during high voltage pulses (60 × 100 V, 1 ms). Only the right part of the plate was exposed, the rest is shown for better clarity. The dimension of the photo is 3.5 × 4.5 mm. Besides some local differences, a complete involvement of the entire skin surface in current flow was evident. The stratum corneum side was pressed against the silver. No broadening of the field lines was responsible for the AgCl-deposition throughout the silver plate. This was extra tested using a polycarbonate membrane with 8 μm holes (Nuclepore™ filter). Here the AgCl-deposition had an average diameter of about 12 μm, which means that the influence radius for AgCl-deposition around a pore was only 2 μm.

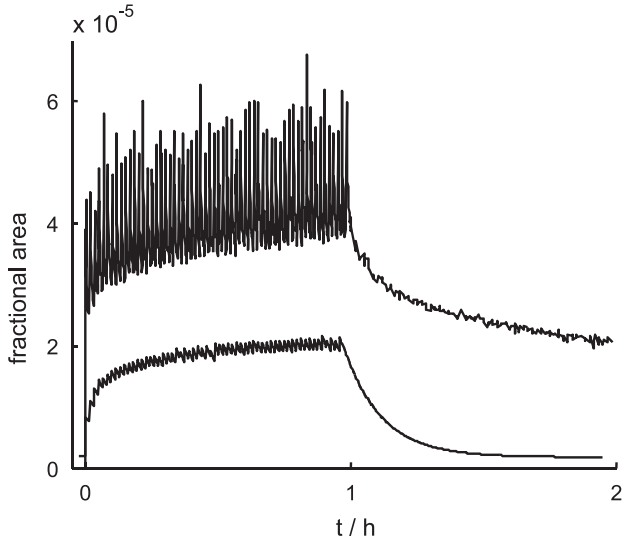

Fig. 3. Fractional area of the stratum corneum involved in transport of small ions (upper curve) and calcein ($M = 623$ g/mol, $z = -4$, lower curve).

which do not recover their electrical resistance. It was also found in earlier studies that the transport of larger molecules like calcein is highly localized in LTR [6]. By comparison of the LTR to the sites where the resistance stayed permanently low, we found a perfect coincidence. Fig. 6 shows the same piece of skin as it was used for the silver plating in Fig. 5 but under fluorescent illumination.

Heating alone could dramatically decrease the resistance of the stratum corneum with the achievement of the phase transition of the skin lipids. The resistance of untreated human stratum corneum was usually between 30 and 500 kΩ cm^2. After heating to 80 °C, the typical resistance was around 200 Ω cm^2. By assuming an LTR coverage of around 10% and using 2 kΩ cm^2 as the post pulse resistance

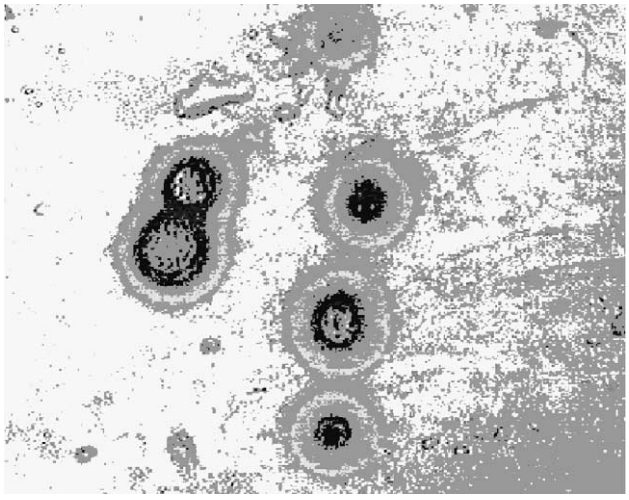

Fig. 4. Silver plate exposed after high voltage pulsing with iontophoretic current (1 min, 100 μA) through the stratum corneum (silver as anode). Most of the silver plate was unaffected, while characteristic spots showed a very high permeability to small ions, indicated by the deposition of silver chloride.

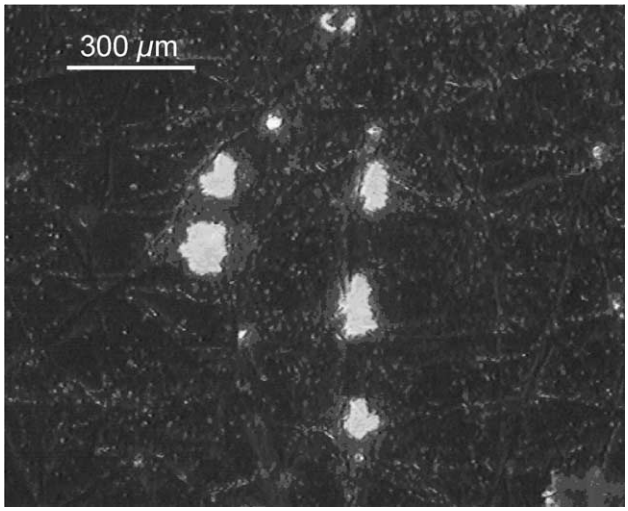

Fig. 5. Fluorescence micrograph of the specimen used in Fig. 4 for silver plating. A high coincidence between the sites where the resistance stayed permanently low and the LTR exists. Moreover, the bright spot above the two LTR at the left-hand side was identified as a sweat duct and showed a resistance by far higher than the LTR. This is in contradiction to unpulsed skin, where sweat ducts and hair follicles were the low resistive pathways through the skin.

of skin treated with sixty 100 V pulses, the resistance of the LTR was on the same order of magnitude as the heated skin. Moreover, high voltage treatment of previously heated skin lowered the resistance even further by an order of magnitude during the presence of the electric field. After the pulse, however, the resistance went back to the pre-pulse value within milliseconds.

3. Discussion

Skin electroporation is not necessarily connected to transdermal molecular transport. Electroporation itself is a two step phenomenon [19]. First, the membranes charge up. Once a critical voltage (breakdown voltage) is exceed for a sufficient time (several microseconds) the creation of aqueous pathways takes place by introduction of water into the lipid bilayer, here the multilamellae of the SC. Macroscopically observed electroporation appears homogeneously throughout the skin. However, there are usually regions with higher energy dissipation, i.e. with a lower resistance during high voltage application. The surface area involved in the transport of small ions reaches up to 0.001 of the entire skin surface. Larger charged molecules, like calcein, are transported in negligible amounts or not at all. Moreover, if the pulse time is less than 10 μs, an almost complete and very fast recovery of the skin resistance happens. The time course of the recovery is comparable to that of BLM. This means, the purely electrically created pores are not the pathways for the passage of large charged species.

With proceeding pulse some spots start to heat up. The number of heated spots is a function of the voltage applied.

During the pulse, heat propagating from the center of the spots causes spot expansion. The reason for these expansions is the probability that additional electroporation at the heated edges of such a spot is higher than the corresponding probability across the bulk stratum corneum. Additional electroporation results in a lower resistance and thus higher energy dissipation at these spots. Heating up the vicinity forces further electroporation and finally generates a propagating heat front. If the energy dissipation is sufficient to exceed the phase transition temperature of the skin lipids (70 °C), then structural changes occur.

The multilamellar lipid system is responsible for the high electric resistance and can become vesicular leaving large aqueous pathways behind [20]. When the electric field is still present, electrophoresis drives charged molecules through the stratum corneum. The degree of the conformational changes of the skin lipids depends on the temperature and the pulse duration. Once the pulse ceases, a fast recovery of the non-heated regions takes place. Here three characteristic times could be distinguished: < 1 ms, 1 s and 10 s [12]. After 10 s, only the LTR exhibited a low resistance value. Since water is not favored in a lipid environment, a partial recovery of the multilamellae could occur. This is the case in the edges of LTR, where the heating time was short and the temperature less. Molecules present in these regions become trapped, yielding the bright ring of the LTR. However, the LTR interior shows a high permeability even for large molecules for at least 30 min. The permeability stays high enough, so that the dye within the center of an LTR is washed away and a dim region remains. As a consequence, elevated ionic permeability starts at the very beginning of electroporation, while the increased permeability to larger, charged species depends on the heat induced structural changes. This alteration of structure is greatly enforced, if the phase transition temperature of the skin lipids is reached. The tremendous enhancement of the transport of charged species is due to the electric field by local electrophoresis. Thus, while the ionic transport sites recovered well, almost no recovery occurred at the molecular transport sites.

4. Conclusion

From a macroscopic point of view, electroporation of stratum corneum usually involves the entire surface. For small ions, the transport surface area for charged species is orders of magnitude less, i.e. 0.001. It is unlikely that the pathways initiated by electroporation are the same pathways for large charged molecule transport. The skin can become permeable for such large charged species only if a synergistic effect between electroporation and Joule heating produces an alteration of the stratum corneum structure. The primary pathways created by electroporation recover fast, while the LTR skin lipid phase transition recovery takes much longer. LTR are the sites of the skin where the phase transition of the skin lipids is exceeded.

Acknowledgements

This work was supported by the Deutsche Forschungsgemeinschaft, Pl 185-2/3. We would like to thank Prof. E. Neumann for useful discussions.

Appendix A. Fractional area for unhindered transdermal flow

The time varying fractional transport area $A(t)$ is the area of unhindered transport with respect to the whole area of the skin specimen A_{total}:

$$A_{\text{f}} = \frac{A(t)}{A_{\text{total}}} \tag{A1}$$

The molar flow $I_i = \mathrm{d}n_i/\mathrm{d}t$ where n_i is the amount of transported molecules of type i and t the time. The flux $J_i = \mathrm{d}I_i/\mathrm{d}A$ is the flow with respect to the transporting surface area A. For practical purposes, we use the definition

$$J_i = \frac{\mathrm{d}n_i}{\mathrm{d}tA_{\text{total}}}. \tag{A2}$$

referring the flow $I_i(t)$ to the total area A_{total}.

The Nernst–Planck equation gives the relationship between the electrochemical driving force and the flux of the substance i through $A(t)$ as:

$$J_i(t) = -D_i\left(\frac{\partial c_i}{\partial x} + \frac{RTc_i}{z_iF}\cdot\frac{\partial \varphi}{\partial x}\right) \tag{A3}$$

where D_i is the diffusion constant for free diffusion in water, R the gas constant, T the absolute temperature, F is the Faraday constant, and z_i is the charge number of i. The actual concentration gradient ($\mathrm{d}c_i/\mathrm{d}x$) within the SC is unknown. Chizmadzhev [14] has proposed a concentration profile shown as dashed line in Fig. 6. However, here we simplify to $\frac{\partial c_i}{\partial x} = \frac{c_{i,\text{receiver}} - c_{i,\text{donor}}}{d_{\text{SC}}}$. Both compartments, the donor

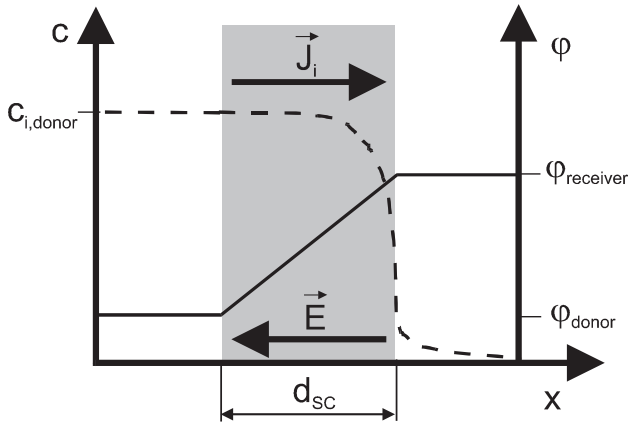

Fig. 6. Concentration profile (c, dashed line) and the electric potential profile (φ, solid line) both as a function of the direction x of the flow vector $\vec{J}_i$. The mean concentration within the stratum corneum is estimated to be c_{donor} [14].

and the receiver were recycled. Hence, $c_{i,\mathrm{donor}}$ is considered as a constant and $c_{i,\mathrm{receiver}}=0$. Therefore, $\frac{\partial c_i}{\partial x}=-\frac{c_{i,\mathrm{donor}}}{d_{\mathrm{SC}}}$.

The potential gradient is approximated by: $\frac{\partial \varphi}{\partial x}=\frac{\varphi_{\mathrm{receiver}}-\varphi_{\mathrm{donor}}}{d_{\mathrm{SC}}}=\frac{\Delta\varphi}{d_{\mathrm{SC}}}=-\frac{U_{\mathrm{SC}}}{d_{\mathrm{SC}}}$.

U_{SC} becomes negative by definition $E=U_{\mathrm{SC}}/d_{\mathrm{SC}}=-\varphi/d_{\mathrm{SC}}$, which is opposite to the direction of the flow vector.

Substitution of the differentials into Eq. (A3) yields:

$$J_i = D_i\left(\frac{c_{i,\mathrm{donor}}}{d_{\mathrm{SC}}}+\frac{RTc_{i,\mathrm{donor}}U_{\mathrm{SC}}}{z_iFd_{\mathrm{SC}}}\right) = \frac{Dc_{i,\mathrm{donor}}}{d_{\mathrm{SC}}}\left(1+\frac{RTU_{\mathrm{SC}}}{z_iF}\right) \quad \text{(A4)}$$

If the flux varies with time, the surface area ($A(t)$) with respect to the total area (A_{total}) changes with time.

$$J_i(t) = \frac{A(t)}{A_{\mathrm{total}}}\frac{Dc_{i,\mathrm{donor}}}{d_{\mathrm{SC}}}\left(1+\frac{RTU_{\mathrm{SC}}}{z_iF}\right) \quad \text{(A5)}$$

yielding Eq. (3) of the text.

Since the transported molecules calcein and sulphorhodamine are negatively charged ($z_{\mathrm{ca}}=-4$, $z_{\mathrm{sr}}=-1$) at pH = 7.4, the voltage $U_{\mathrm{sc}}=\varphi_{\mathrm{donor}}-\varphi_{\mathrm{receiver}}$ is negative, the term z_iU_{SC} becomes positive driving the molecules along the electric field (Fig. 6).

References

[1] M.E. Johnson, D.A. Berk, D. Blankenstein, D.E. Golan, R.K. Jain, R. Langer, Lateral diffusion of small compounds in human stratum corneum and model lipid bilayer systems, Biophys. J. 71 (1996) 2656–2668.

[2] S. Mitragotri, D. Blankenstein, R. Langer, Ultrasound-mediated transdermal protein delivery, Science 269 (1995) 850–853.

[3] E. Neumann, A. Sowers, C. Jordan, Electroporation and Electrofusion in Cell Biology, Plenum Press, New York, 1989.

[4] M.R. Prausnitz, V.G. Bose, R. Langer, J.C. Weaver, Electroporation of mammalian skin: a mechanism to enhance transdermal drug delivery, Proc. Natl. Acad. Sci. U. S. A. 90 (1993) 10504–10508.

[5] U. Pliquett, J.C. Weaver, Electroporation of human skin: simultaneous measurement of changes in the transport of two fluorescent molecules and in the passive electrical properties, Bioelectrochem. Bioenerg. 39 (1996) 1–12.

[6] U. Pliquett, T.E. Zewert, T. Chen, R. Langer, J.C. Weaver, Imaging of fluorescent molecule and small ion transport through human stratum corneum during high-voltage pulsing: localized transport regions are involved, Biophys. Chem. 58 (1996) 185–204.

[7] M.R. Prausnitz, J.A. Gimm, R.H. Guy, R. Langer, J.C. Weaver, C. Cullander, Imaging regions of transport across human stratum corneum during high voltage and low voltage exposures, J. Pharm. Sci. 85 (1996) 1363–1370.

[8] U. Pliquett, R. Vanbever, J.C. Weaver, Local transport regions (LTRs) in human stratum corneum due to long and short high voltage pulses, Bioelectrochem. Bioenerg. 47 (1998) 151–161.

[9] M.R. Prausnitz, C.S. Lee, C.H. Liu, J.C. Pang, T.P. Singh, R. Langer, J.C. Weaver, Transdermal transport efficiency during skin electroporation and iontophoresis, J. Control. Release 38 (1996) 205–217.

[10] M.R. Prausnitz, U. Pliquett, R. Vanbever, Mechanistic studies of skin electroporation using biophysical methods, in: M. Jaroszeski, R. Gilbert, R. Heller (Eds.), Electrically Mediated Delivery of Molecules to Cells: Electrochemotherapy, Electrogenetherapy, and Transdermal Drug Delivery by Electroporation, Humana Press, Totowa, 1999, pp. 213–246.

[11] C.L. Gummer, The in vitro evaluation of transdermal delivery, in: J. Hadgraft, R.H. Guy (Eds.), Transdermal Drug Delivery: Development Issues and Research Initiatives, Marcel Dekker, New York, 1989, pp. 177–186.

[12] U. Pliquett, R. Langer, J.C. Weaver, Changes in the passive electrical properties of human stratum corneum due to electroporation, Biochim. Biophys. Acta 1239 (1995) 111–121.

[13] U. Pliquett, M.R. Prausnitz, Electrical impedance spectroscopy for rapid and non-invasive analysis of skin electroporation, in: M. Jaroszeski, R. Gilbert, R. Heller (Eds.), Electrically Mediated Delivery of Molecules to Cells: Electrochemotherapy, Electrogenetherapy, and Transdermal Drug Delivery by Electroporation, Humana Press, Totowa, 1999, pp. 377–406.

[14] Y.A. Chizmadzhev, V.G. Zarnitsin, J.C. Weaver, R.O. Potts, Mechanism of electroinduced ionic species transport through a multilamellar lipid system, Biophys. J. 68 (1995) 749–765.

[15] G. Adam, P. Lauger, G. Stark, Biophysikalische Chemie und Biophysik, Springer Verlag, Heidelberg, 1995.

[16] U. Pliquett, J.C. Weaver, Transport of a charged molecule across the human epidermis due to electroporation, J. Control. Release 38 (1996) 1–10.

[17] U. Pliquett, C. Gusbeth, Perturbation of human skin due to application of high voltage, Bioelectrochem. Bioenerg. 51 (2000) 41–51.

[18] U. Pliquett, M.R. Prausnitz, Y.A. Chizmadzhev, J.C. Weaver, Measurement of rapid release kinetics for drug delivery, Pharm. Res. 12 (1995) 549–555.

[19] R.W. Glaser, S.L. Leikin, L.V. Chernomordik, V.F. Pastuchenko, A.I. Sokirko, Reversible electrical breakdown of lipid layers: formation and evolution of pores, BBA 940 (1988) 275–287.

[20] S.A. Gallo, A. Sen, M.L. Hensen, S.W. Hui, Temperature-dependent electrical and ultrastructural characterization of porcine skin upon electroporation, Biophys. J. 82 (2002) 109–119.